Expert Systems with Applications 39 (2012) 6720–6728

Contents lists available at SciVerse ScienceDirect

Expert Systems with Applications

journal homepage: www.elsevier.com/locate/eswa

Gaussian mixture modeling of histograms for contrast enhancement

Yu-Ren Lai, Kuo-Liang Chung *,[1], Guei-Yin Lin, Chyou-Hwa Chen

Department of Computer Science and Information Engineering, National Taiwan University of Science and Technology, No. 43, Section 4, Keelung Road, Taipei 10672, Taiwan, ROC

ARTICLE INFO

Keywords:
Contrast enhancement
Expectation maximization
Gaussian mixture model
Histogram equalization
K-means

ABSTRACT

The current major theme in contrast enhancement is to partition the input histogram into multiple sub-histograms before final equalization of each sub-histogram is performed. This paper presents a novel contrast enhancement method based on Gaussian mixture modeling of image histograms, which provides a sound theoretical underpinning of the partitioning process. Our method comprises five major steps. First, the number of Gaussian functions to be used in the model is determined using a cost function of input histogram partitioning. Then the parameters of a Gaussian mixture model are estimated to find the best fit to the input histogram under a threshold. A binary search strategy is then applied to find the intersection points between the Gaussian functions. The intersection points thus found are used to partition the input histogram into a new set of sub-histograms, on which the classical histogram equalization (HE) is performed. Finally, a brightness preservation operation is performed to adjust the histogram produced in the previous step into a final one. Based on three representative test images, the experimental results demonstrate the contrast enhancement advantage of the proposed method when compared to twelve state-of-the-art methods in the literature.

1. Introduction

Contrast enhancement stretches the dynamic range of an image to make use of the full spectrum of possible gray values (Gonzalez & Woods, 2002) and has been found to be useful for an extremely wide range of applications, such as texture synthesis (Pei, Zeng, & Chang, 2004), threshold determination in noise removal (Ghanekar, Singh, & Pandey, 2010), medical image diagnosis (Li, Wang, & Yu, 1994; Pizer, 2003; Zimmerman et al., 1988), fingerprint recognition (Wahab, Chin, & Tan, 1998), speech recognition (Torre et al., 2005), electrophoretic displays (Kao, Ye, Chu, & Su, 2009), tone mapping technique (Kang, Kim, & Sohn, 2009), and so on.

Many contrast enhancement methods have been proposed in the literature. Histogram equalization (HE) (Gonzalez & Woods, 2002) is the earliest and simplest contrast enhancement method by mapping the probability distribution of gray values to a uniform probability distribution. Unfortunately, HE causes many types of undesirable artifacts. For example, some regions in the resultant image may appear to be overexposed while others underexposed. In addition, the resultant images often do not have the same mean brightness as the original ones. To improve brightness-preservation, Kim (1997) presented an extended HE, called the mean preserving bi-histogram equalization (BBHE) method, in which the mean gray value is taken as the pivot used to partition the image into two sub-images. The sub-image with smaller gray values is mapped into the range from the minimum gray level of the input image to the pivot and the sub-image with larger gray values is mapped into the range from the pivot to the maximum gray level of the input image. Instead of using the mean gray value as the pivot to partition the input image, Wang, Chen, and Zhang (1999) presented an equal area dualistic sub-image-based HE (DSIHE) to partition the original image into two sub-images such that each sub-image has equal cumulative probability density function. The recursive mean-separate HE (RMSHE) proposed by Chen and Ramli (2003) is another effort that improved the BBHE. The minimum mean brightness error bi-HE (MMBEBHE) proposed by Chen and Ramli (2003) is an extension of BBHE that provides maximal brightness preservation. Sim, Tso, and Tan (2007) generalized the DSIHE into Recursive sub-image HE (RSIHE). The difference between the RSIHE and the DSIHE is that the median-based histogram segmentation is adopted once in the DSIHE, but it is adopted several times in the RSIHE.

Wadud, Kabir, Dewan, and Chae (2007) presented a dynamic HE (DHE) in which the input image is partitioned into sub-histograms based on local minimum; next, sub-histogram is re-split if its distribution is not normal, and finally, a gray level range allocation to sub-histogram is performed. Ibrahim and Kong (2007) presented a brightness preserving DHE (BPDHE). First, the BPDHE smoothes the input histogram using a 1-D Gaussian filter, and then it partitions the smoothed histogram based on its local maximums. Each parti-

* Corresponding author.
E-mail address: k.l.chung@mail.ntust.edu.tw (K.-L. Chung).

[1] This work is supported by National Science Council of ROC under contract NSC98-2221-E-011-084-MY3.

0957-4174/$ - see front matter © 2011 Elsevier Ltd. All rights reserved.
doi:10.1016/j.eswa.2011.12.018

tion is then assigned to a new dynamic range and the HE will alter the mean brightness to achieve the brightness preserving effect. Recently, Sengee and Choi (2008) presented a brightness preserving weight clustering HE (BPWCHE). Kim and Chung (2008) presented a recursively separated and weighted HE (RSWHE). Basically, RSWHE is similar to RSIHE and RMSHE, but RSWHE has the weighting process which leads to better contrast enhancement and brightness preserving effect. Currently, Ibrahim and Kong (2009) presented sub-regions histogram equalization (SRHE) which not only can enhance the contrast, but it also sharpens the image. Next, Hashemi, Kiani, Noroozi, and Moghaddam (2010) presented a contrast enhancement method based on the genetic algorithm. The genetic based contrast enhancement method, called the GHE, utilizes an array to sort random integer numbers, and the gray values of the histogram are mapped according these random integer numbers. Finally, Cheng, Xue, Shi, and Zhang (2007) proposed a contrast enhancement method based on the fuzzy theory. This fuzzy based contrast enhancement method, called the FHE, uses the fuzzy homogeneity to enhance the contrast of the image.

It can be seen from the discussions of related works that the current major theme in contrast enhancement is to partition the input histogram into multiple sub-histograms before final equalization of each sub-histogram is performed. This paper presents a novel contrast enhancement method based on Gaussian mixture modeling of image histograms, which provides a sound theoretical underpinning of the partitioning process. The contrast enhancement method we propose is called EMCE+BP. Our method comprises five major steps. First, the number of Gaussian functions to be used in the model is determined using a cost function of input histogram partitioning. Then the parameters of a Gaussian mixture model are estimated to find the best fit to the input histogram under a threshold associated with an error bound. A binary search strategy is then applied to find the intersection points between the Gaussian functions. The intersection points thus found are used to partition the input histogram into a new set of sub-histograms, on which the classical histogram equalization (HE) is performed. Finally, a brightness preservation operation is performed to adjust the histogram produced in the previous step into a final one. Based on three representative test images, we compare the performance of EMCE+BP with twelve existing methods, including HE, BBHE, RMSHE, DSIHE, RSIHE, DHE, BPDHE, RSWHE, BPWCHE, SRHE, GHE, and FHE using both objective and subjective evaluation. The objective measure considers EME (Agaian, Panetta, & Grigoryan, 2000) and algorithm execution time. The subjective evaluation involves detailed examination of the output images visually. The experimental results demonstrate the superiority of our method when compared to the other methods.

The rest of this paper is organized as follows. In Section 2, the proposed EMCE+BP method is presented. In Section 3, experimental results are presented to illustrate the contrast enhancement advantage of our proposed method. In Section 4, we discuss the conclusions of this work.

2. The proposed method

As discussed before, our method comprises of five major steps. First, the number of Gaussian functions to be used in the model is determined using a cost function of input histogram partitioning. Then the parameters of a Gaussian mixture model are estimated to find the best fit to the input histogram under a threshold error bound. A binary search strategy is then applied to find the intersection points between the Gaussian functions. The intersection points thus found are used to partition the input histogram into a new set of sub-histograms, on which the classical histogram equalization (HE) is performed. Finally, a brightness preservation operation is performed to adjust the histogram produced in the previous step into a final one. In the following, we describe the five major steps in details.

2.1. Determination of the number of Gaussian functions in the mixture

Let the range of gray values for an image lies between 0 and L. The value of L is usually 255. Let i, n_i, and N indicate the gray level, $0 \leqslant i \leqslant L$, the number of pixels (or frequency) with gray level i, and the total number of pixels in I, respectively. The probability of n_i over N is defined by $p_i = n_i/N$.

Given the histogram of an input image I, we need to determine the value K, into which the histogram will be partitioned into sub-histograms. Let $t_1, t_2, \ldots$, and $t_K - 1$ be the $K-1$ thresholds that partition the histogram into K sub-histograms with $2 \leqslant K \leqslant L$. Let C_i denote the set of gray values of the ith sub-histogram, $1 \leqslant i \leqslant K$. That is, $C_i = \{t_i - 1 + 1, t_i - 1 + 2, \ldots, t_i\}$.

For the K sub-histograms, the probability for each sub-histogram C_j, $1 \leqslant j \leqslant K$, is calculated by

$$\omega_1(t_1) = \sum_{i=0}^{t_1} P_i, \omega_2(t_2) = \sum_{i=t_1+1}^{t^2} P_i, \ldots, \omega_K(t_K) = \sum_{i=t_K-1+1}^{L} P_i, \tag{1}$$

Obviously, $\omega_1(t_1) + \omega_2(t_2) + \cdots + \omega_K(t_K) = 1$.

Based on Eq. (1), the mean for each of the K sub-histograms is calculated by

$$\begin{aligned}\mu_1(t_1) &= \sum_{i=0}^{t_1} \frac{iP_i}{\omega_1(t_1)}, \mu_2(t_2) = \sum_{i=t_1+1}^{t_2} \frac{iP_i}{\omega_2(t_2)}, \ldots, \mu_K(t_K) \\ &= \sum_{i=t_{K-1}+1}^{L} \frac{iP_i}{\omega_K(t_K)},\end{aligned} \tag{2}$$

Similarly, based on Eq. (2), the variance for each of these sub-histograms is calculated by

$$\begin{aligned}\sigma_1(t_1) &= \sum_{i=0}^{t_1} (i - \mu_1(t_1))^2 \frac{P_i}{\omega_1(t_1)}, \sigma_2(t_2) \\ &= \sum_{i=t_1+1}^{t_2} (i - \mu_2(t_2))^2 \frac{P_i}{\omega_2(t_2)}, \ldots, \sigma_K(t_K) \\ &= \sum_{i=t_{K-1}+1}^{L} (i - \mu_K(t_K))^2 \frac{P_i}{\omega_K(t_K)},\end{aligned} \tag{3}$$

The quality of a partitioning scheme is partially judged by the variance of a partitioning scheme. Clearly, a partitioning scheme whose variance is small is preferable to another one with a large variance. Based on Eqs. (1) and (3), the variance of a histogram partition scheme is defined by

$$\sigma_\omega^2 = \sum_{i=1}^{K} \omega_i(t_i)\sigma_i^2(t_i), \tag{4}$$

However, the quality of a partitioning scheme cannot be determined by the variance of a partitioning scheme alone, since the best partitioning scheme is trivially the one with L sub-histograms. Therefore, we define the quality of a partitioning scheme using the cost function

$$Cost = K(\log_2 K) + \lambda\sigma_\omega, \tag{5}$$

According to Eq. (5), the cost of a partitioning scheme is a balance between the standard derivation σ_ω and the number of sub-histograms. We have found that the Lagrange multiplier λ with 1.5 performs well empirically. To find the best K value, an iterative algorithm is obtained. The algorithm starts from $K = 1$ onwards. In each iterative, the cost function is evaluated. When the value of the cost function reaches the first local minimum, the algorithm

stops. In this manner, the number of Gaussian functions, K, to be used in the GMM model is determined.

2.2. Estimating the parameters of the Gaussian mixture model (GMM)

We regard the image histogram as a Gaussian mixture model (GMM) (Xu & Jordan, 1996), which is a parametric statistical model that assumes that the data originates from a weighted sum of several Gaussian functions. In the model, the probability of the pixel gray value x_i, $0 \leqslant i \leqslant N-1$, with respect to the j^{th} Gaussian function is defined as

$$g(x_i, \mu_j, \sigma_j) = \frac{1}{\sqrt{2\pi\sigma_j^2}} exp\left(\frac{-(x_i-\mu_j)^2}{2\sigma_j^2}\right). \quad (6)$$

The overall mixture model for x_i is a weighted summation of the individual Gaussian functions, and is defined as follows.

$$p(x_i) = \sum_{j=1}^{K} \alpha_j g(x_i, \mu_j, \sigma_j), \quad (7)$$

where α_j denotes the weight of the jth Gaussian function and $\alpha_1 + \alpha_2 + \cdots + \alpha_K$ is held. A popular efficient iterative algorithm to estimate the set of relevant statistical parameters in Eq. (7) is the EM algorithm (Hartley, 1958). In order to compute the optimal θ, the EM algorithm iteratively updates the $3K$ parameters until the likelihood function in Eq. (8) is maximized.

$$J(\theta) = \ln\left[\prod_{i=0}^{N-1} p(x_i)\right] = \prod_{i=0}^{N-1} \ln p(x_i). \quad (8)$$

In the EM, to find the maxima of $J(\theta)$, the function is differentiated at α_j,μ_j, and σ_j, and set to zero. This yields a new set of parameters for the mixture model, as shown in the following equations.

$$\alpha_j = \frac{1}{N}\sum_{i=0}^{N-1}\left(\frac{\alpha_j g(x_i, \mu_j, \sigma_j)}{\sum_{l=1}^{K}\alpha_l g(x_i, \mu_l, \sigma_l)}\right), \quad (9)$$

$$\mu_j = \frac{\sum_{i=0}^{N-1}\left(\frac{\alpha_j g(x_i,\mu_j,\sigma_j)}{\sum_{l=1}^{K}\alpha_l g(x_i,\mu_l,\sigma_l)}\right)x_i}{\sum_{i=0}^{N-1}\left(\frac{\alpha_j g(x_i,\mu_j,\sigma_j)}{\sum_{l=1}^{K}\alpha_l g(x_i,\mu_l,\sigma_l)}\right)}, \quad (10)$$

$$\sigma_j^2 = \frac{\sum_{i=0}^{N-1}\left(\frac{\alpha_j g(x_i,\mu_j,\sigma_j)}{\sum_{l=1}^{K}\alpha_l g(x_i,\mu_l,\sigma_l)}\right)(x_i-\mu_j)^2}{\sum_{i=0}^{N-1}\left(\frac{\alpha_j g(x_i,\mu_j,\sigma_j)}{\sum_{l=1}^{K}\alpha_l g(x_i,\mu_l,\sigma_l)}\right)}. \quad (11)$$

The above operations are performed iteratively until it converges. In more details, the EM algorithm consists of the following five steps.

Step 1: Compute the initial parameters θ where $\alpha_j = \frac{1}{K}$; μ_j and $\sigma_j^2, 1 \leqslant j \leqslant K$, have been computed by the method mentioned in Section 2.1. (Based on the partitioned histogram with K sub-histogram, for each sub-histogram $C_j, 1 \leqslant j \leqslant K$, its mean μ_j and variance σ_j^2 are first calculated.)
Step 2: By Eq. (10), compute the new μ_j as $\mu_{j,new}$.
Step 3: By Eq. (11), compute the new σ_j^2 as $\sigma_{j,new}^2$.
Step 4: By Eq. (9), compute the new α_j as $\alpha_{j,new}$.
Step 5: Let $\theta_{new} = \{\alpha_{1,new}, \alpha_{2,new}, \ldots, \alpha_{K,new}, \mu_{1,new}, \mu_{2,new}, \ldots, \mu_{K,new}, \sigma_{1,new}^2, \sigma_{2,new}^2, \ldots, \sigma_{K,new}^2\}$. If $|\theta - \theta_{new}| < T$, where the threshold T is a parameter and empirically T is set to 10^{-3}, then stop; otherwise, let $\theta - \theta_{new}$ and go to Step 2.

At the end of the EM iterative algorithm, the parameters to the GMM model $\theta_{end} = \{\alpha_{1,end}, \alpha_{2,end}, \ldots, \alpha_{K,end}, \mu_{1,end}, \mu_{2,end}, \ldots, \mu_{K,end}, \sigma_{1,end}^2, \sigma_{2,end}^2, \ldots, \sigma_{K,end}^2\}$ are determined. The intersection points between the Gaussian functions in the mixture model are used as thresholds for histogram partitioning. How to do that is described in the next subsection.

2.3. Determination of intersection points between adjacent Gaussian functions

In this subsection, a binary search strategy is presented to determine the intersection points between adjacent Gaussian functions. Fig. 1 illustrates the idea of the proposed strategy.

There are two cases to consider. In case 1, two adjacent Gaussian functions do not cover each other. This happens when $\alpha_{j+1}g(\mu_{j+1}, \mu_{j+1}, \sigma_{j+1}) > \alpha_j g(\mu_{j+1}, \mu_j, \sigma_j)$ and $\alpha_j g(\mu_j, \mu_j, \sigma_j) > \alpha_{j+1} g(\mu_j, \mu_{j+1}, \sigma_{j+1})$.

In case 2, one Gaussian function is covered by the other one. This case is further divided into two sub-cases. The first subcase, b1, of case 2 happens when $\alpha_j g(\mu_{j+1}, \mu_j, \sigma_j) > \alpha_{j+1} g(\mu_{j+1}, \mu_{j+1}, \sigma_{j+1})$ and $\alpha_j g(\mu_j, \mu_j, \sigma_j) > \alpha_{j+1} g(\mu_j, \mu_{j+1}, \sigma_{j+1})$, it is sub-case b1 in case 2. The second subcase, b2, of case 2 happens when $\alpha_{j+1}g(\mu_{j+1}, \mu_{j+1}, \sigma_{j+1}) > \alpha_j g(\mu_{j+1}, \mu_j, \sigma_j)$ and $\alpha_{j+1} g(\mu_j, \mu_{j+1}, \sigma_{j+1}) > \alpha_j g(\mu_j, \mu_j, \sigma_j)$.

The algorithm for finding the intersection points between adjacent Gaussian functions is shown in the following. Due to limitation on paper length, we only discuss case 1 and sub-case b1 in the algorithm. Sub-case b2 follows similar reasoning and is not discussed further.

```
1.  Procedure 1: Compute intersection points
2.  Case 1: p ← DetermineIntersectionPoint (μ_j, μ_{j+1})
3.  Case 2: midPoint ← (μ_j, μ_{j+1})/2
4.  if (α_{j+1}g(midPoint, μ_{j+1}, σ_{j+1}) > α_j g(mid_point, μ_j, σ_j))
5.    p_1 ← DetermineIntersectionPoint(0, μ_j)
6.  else
7.    p_2 ← DetermineIntersectionPoint(μ_{j+1}, 255)
8.  ==========
9.  DetermineIntersectionPoint(μ_j, μ_{j+1})
10. {  midPoint ← (μ_j, μ_{j+1})/2
11.   prob_j ← α_j g(midPoint, μ_j, σ_j)
12.   prob_{j+1} ← α_{j+1} g(midPoint, μ_{j+1}, σ_{j+1})
13.   if (abs(prob_j − prob_{j+1}) < threshold) then
14.     return midPoint
15.   else
16.   {  if (abs(prob_j > prob_{j+1})) then
17.       DetermineIntersectionPoint (midPoint, μ_{j+1})
18.     else
19.       DetermineIntersectionPoint (μ_j, midPoint)  }  }
```

For case 1, we now describe how to determine the intersection point p. Let $m_0 = (\mu_j + \mu_{j+1})/2$ be the first mid-point. If $\alpha_j g(m_0, \mu_j, \sigma_j) > \alpha_{j+1} g(m_0, \mu_{j+1}, \sigma_{j+1})$, $m_1 = (m_0 + \mu_{j+1})/2$ is used as the second mid-point; otherwise, $m_1 = (m_0 + \mu_j)/2$ is used as the second mid-point. We repeat the above binary search-based process until the distance between two consecutive mid-points, say $\overline{m_t}$ and $\overline{m_{t+1}}$, is small enough. At that time, $p = (\overline{m_t} + \overline{m_{t+1}})/2$ is used as the determined intersection point of $\alpha_j g(x_i, \mu_j, \sigma_j)$ and $\alpha_{j+1} g(x_i, \mu_{j+1}, \sigma_{j+1})$.

For sub-case b1 in case 2, in order to find the right intersection point p_2, $m_1 = (\mu_{j+1} + 255)/2$ is used as the second mid-point. If $\alpha_j g(m, \mu_j, \sigma_j) > \alpha_{j+1} g(m, \mu_{j+1}, \sigma_{j+1})$, $m_2 = (m_1 + 255)/2$ is used as the third mid-point; otherwise, $m_2 = (m_1 + \mu_{j+1})/2$ is used as the third mid-point. The above binary search process is repeated until the distance between two consecutive mid-points is small enough. Consequently, the mean of the two consecutive mid-points is taken

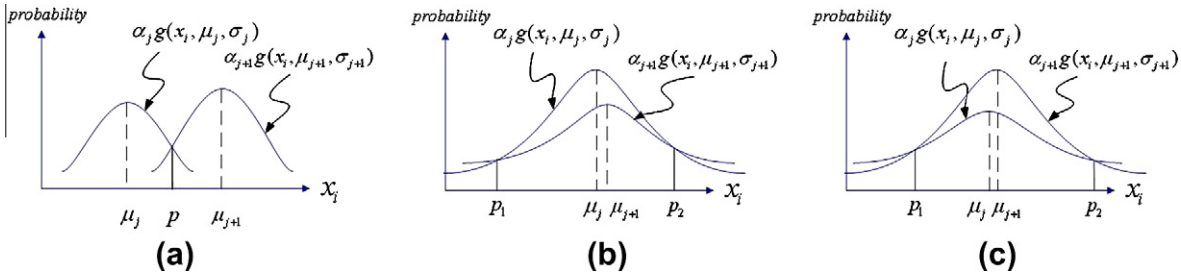

Fig. 1. Two cases for determining intersection points between two adjacent Gaussian functions. (a) Case 1: non-covering case. (b) Case 2: two covering sub-cases, b1 and b2.

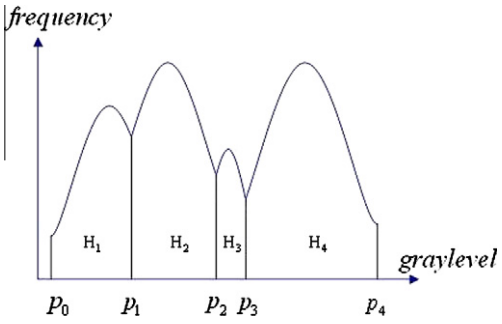

Fig. 2. Segmented histogram with four sub-histograms.

as the right intersection point p_2. By the same arguments, the left intersection point p_1 can be found. Procedure 1 is used to realize the above proposed intersection point finding scheme where the value of the threshold $T_i p$ in Procedure 1 is specified to 0.06, which will be discussed in Section 3.

At the end of the algorithm, the determined intersection points are used as thresholds to re-partition the original histogram into K' sub-histogram, where K' denotes the number of determined intersection points. As an example in case $K' = 3$, the intersection points, $p_1, p_2, \ldots$, and p_3, are used as thresholds to partition the image histogram into four sub-histograms as shown in Fig. 2.

2.4. Application of HE to each sub-histogram for contrast enhancement

After the original image histogram is partitioned into sub-histograms in the previous step, HE is applied to each sub-histogram for

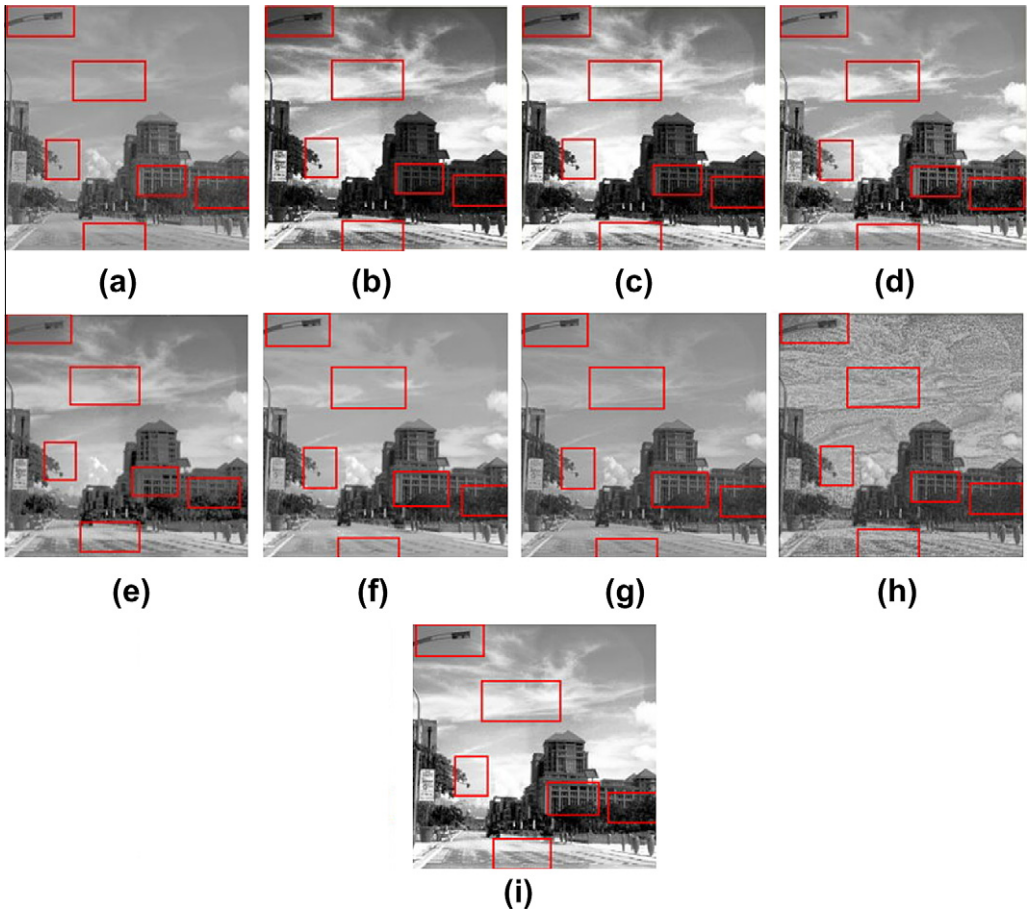

Fig. 3. For image "*Putrajaya*", the results by using non-mean preserving-based methods. (a) Original image. (b) HE. (c) DSIHE. (d) RSIHE. (e) DHE. (f) GHE. (g) FHE. (h) SRHE. (i) The proposed EMCE.

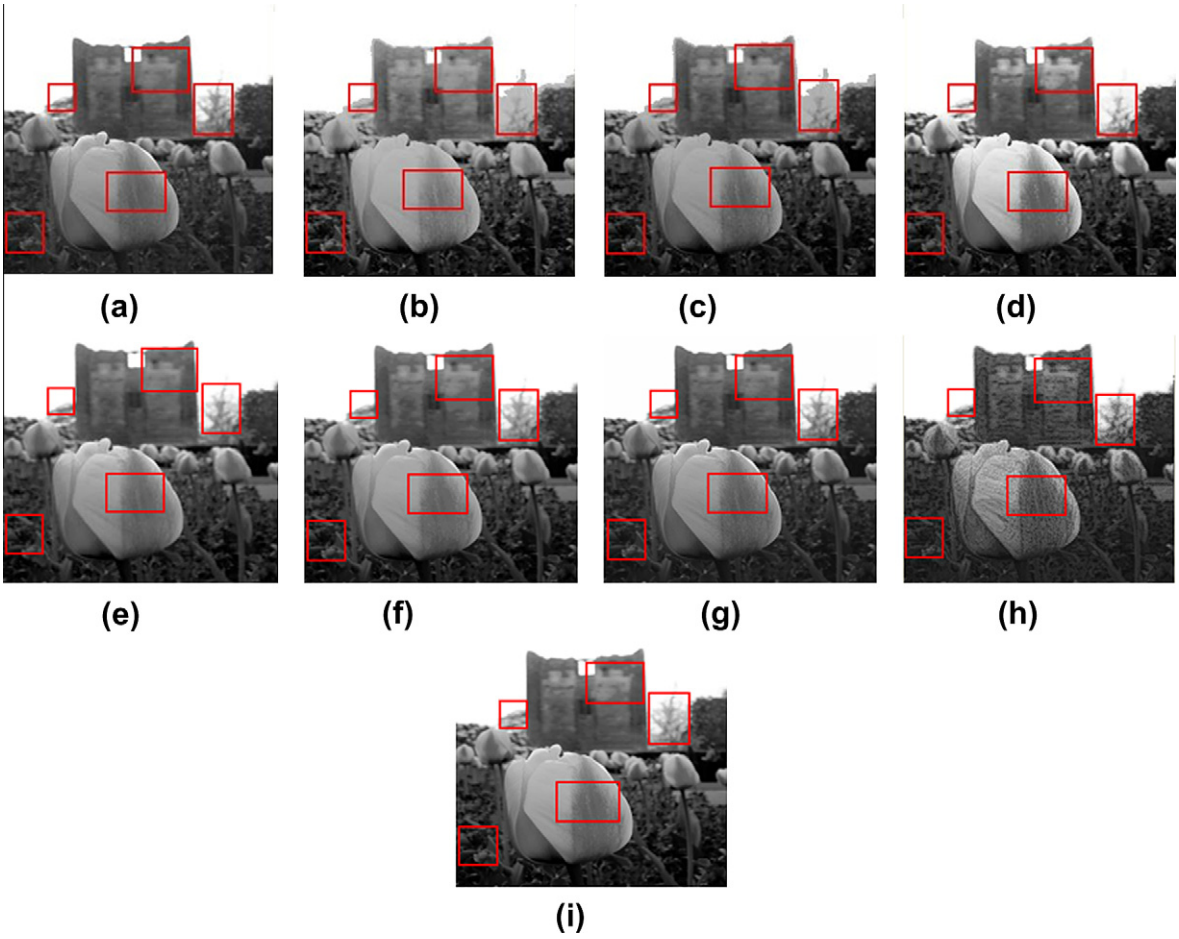

Fig. 4. For image "*Castle*", the results by using non-mean preserving-based methods. (a) Original image. (b) HE. (c) DSIHE. (d) RSIHE. (e) DHE. (f) GHE. (g) FHE. (h) SRHE. (i) The proposed EMCE.

contrast enhancement. For example, in Fig. 2, the sub-histograms $H1$, $H2$, $H3$, and $H4$ are equalized using HE individually.

2.5. Brightness preservation operation

In order to achieve brightness preservation, the histogram produced in the previous step is modified in the following manner. We first compute the mean gray level of the sub-histograms, say $mean_s$, and compute the difference between $mean_s$ and the mean of the original input image. Next, the difference is added to each pixel in the enhanced image to achieve brightness preservation.

In order to have a fair comparison between these methods and ours, we will also present results pertaining to a non-brightness preserving variant of EMCE+BP, called EMCE. The proposed EMCE is simply EMCE+BP excluding the brightness preservation operation.

3. Experimental results

We have compared the performance of EMCE+BP and EMCE with twelve other state-of-the-art methods. The relevant methods may be divided into two groups, depending on whether brightness preservation is performed. In general, the brightness preserving methods operate in a more restricted dynamic range. The difference in whether brightness preservation is desired has a significant impact on the performance of a contrast enhancement method. The brightness preserving methods include BBHE, RMSHE, BPDHE, RSWHE, BPWCHE, and our EMCE+BP method. The non-brightness preserving methods include HE, DSIHE, RSIHE, DHE, SRHE, GHE, FHE, and our proposed EMCE method.

The contrast enhancement performance comparison among the relevant methods are done using both objective and subjective evaluation. For objective evaluation, the EME measure, which is proposed by Agaian et al. (2000), is used. For subjective evaluation, detailed examination of the output images are performed.

The EME measure is defined as follows

$$EME = \frac{1}{K_1 K_2} \sum_{i=1}^{K_1} \sum_{j=1}^{K_2} 20 \times \ln \frac{I_{max;i,j}}{I_{min;i,j} + c}, \tag{12}$$

where the test image is broken up into $K_1 K_2$ blocks, and $I_{max;i,j}$ and $I_{min;i,j}$ are the maximum and minimum intensities in a given block. This contrast enhancement measure is used to find the average ratio of maximum to minimum intensities in the resultant image.

The objective and subjective comparison of the relevant methods have been performed using three representative images, *Putrajaya*,*Castle*, and *Aircraft*, shown in Fig. 3(a), Fig. 4(a), and Fig. 5(a), respectively. In addition, we have compared the execution time of the relevant methods. All of the compared methods are implemented using Borland C++ Builder 6.0 and run on a standard PC with AMD Athlon 64 × 2 4800+CPU (2.5 GHz) and 1.87 GB of RAM.

The experimental results are presented in four sets. First, we present the objective comparison results for all the methods in terms of execution time and the objective EME measure. Detailed subjective examination of the resulting contrast enhanced images

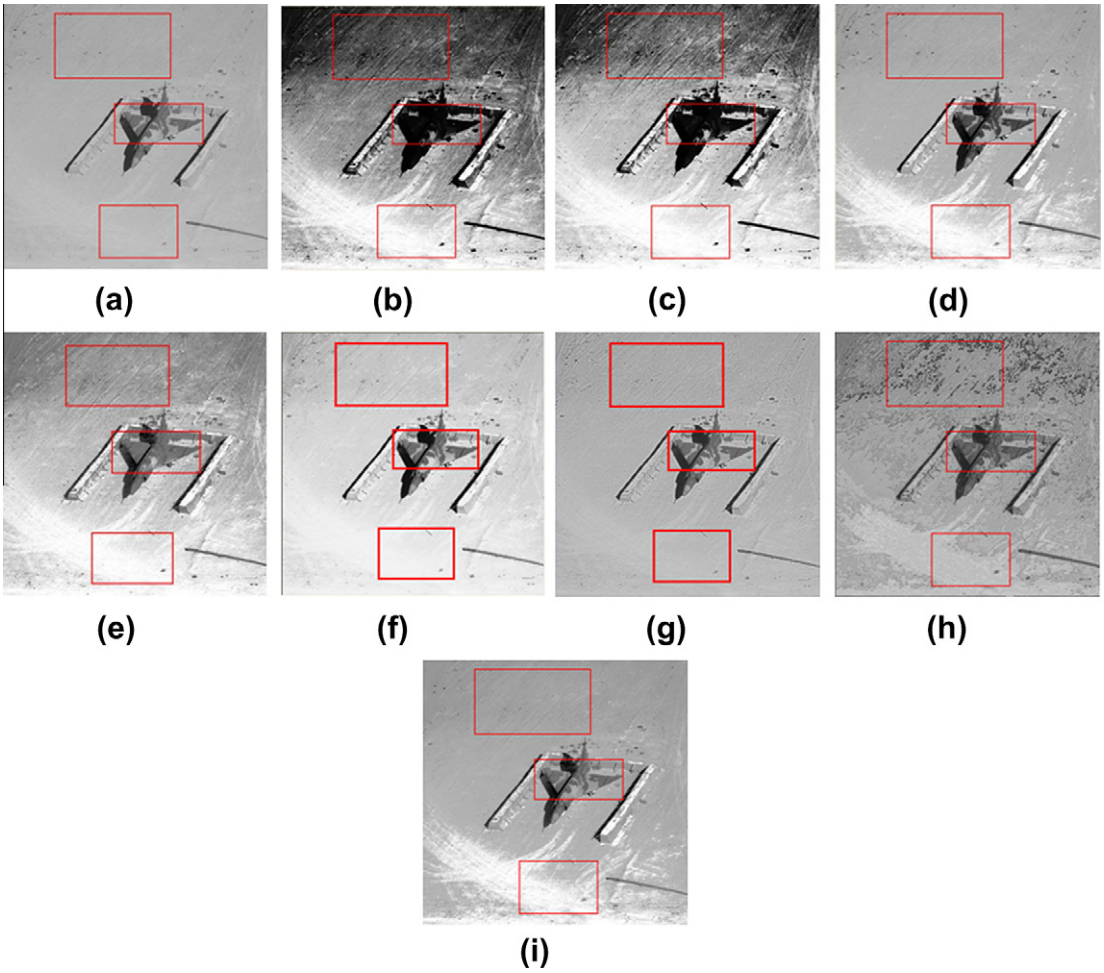

Fig. 5. For image "*Aircraft*", the results by using non-mean preserving-based methods. (a) Original image. (b) HE. (c) DSIHE. (d) RSIHE. (e) DHE. (f) GHE. (g) FHE. (h) SRHE. (i) The proposed EMCE.

for non-brightness preserving methods are then presented. The same examination is then performed for brightness preserving methods. Finally, we investigate the impact of the T_{ip} parameter on the performance of our method.

3.1. Objective comparison of all the methods

Table 1 lists the objective contrast enhancement EME measure results for all of the methods. In Table 1, when compared with the other twelve methods, the results demonstrate that EMCE+BP has the highest average EME measure values. This indicates that the contrast enhanced images produced by EMCE+BP are the most contrasty. With respect to the average EME value performance for EMCE, even though it does not achieve the highest average value, its subjective contrast enhancement performance of the proposed EMCE is superior to other compared methods, as will be shown later.

With respect to the execution time in terms of seconds, the results are shown in Table 2. Table 2 indicates that all compared algorithms are very efficient, except for SRHE and FHE, which are significantly more time consuming than other methods.

Table 1
For three test images, the comparison of all concerned methods in terms of EME measure.

Methods	EME			Average EME
	Putrajaya	*Aircraft*	*Castle*	
HE	26.35	**29.949**	18.481	24.9267
DSIHE	25.165	27.281	20.483	24.3097
RSIHE	21.858	19.399	19.43	20.229
DHE	6.696	5.926	9.627	7.41633
GHE	9.457	6.581	14.368	10.1353
FHE	8.183	7.571	10.752	8.83533
SRHE	12.301	23.97	14.226	16.8323
BBHE	22.56	26.105	18.738	22.4677
RSWHE	10.125	7.106	13.149	10.1267
BPDHE	12.088	8.947	13.215	11.4167
BPWCHE	7.558	5.633	8.994	7.395
RMSHE	27.6	14.106	32.76	24.822
The proposed EMCE	24.662	10.173	22.063	18.966
The proposed EMCE+BP	**58.463**	15.503	**24.769**	**32.911**

3.2. Subjective comparison of non-brightness preserving methods

In this subsection, we compare the performance of the non-brightness preserving methods, the EMCE, the HE, the DSIHE, the RSIHE, the DHE, the SRHE, the GHE, and the FHE, using three representative test images. For the first test image "*Putrajaya*", Fig. 3 indicates that the RSIHE and our proposed EMCE have good contrast, especially on the streetlamp located at the left side of the image. The resultant images produced by the two methods, the HE and the DSIHE, are too dark. The resultant images produced by the DHE, the SRHE, the GHE, and the FHE show blurriness on the windows.

Table 2
The execution time requirement in terms of seconds.

Methods	HE	BBHE	RMSHE	RSIHE	DSIHE	BPDHE	BPWCHE	DHE
Execution time (*s*)	0.0155	0.0155	0.0157	0.0187	0.0189	0.0219	0.0235	0.0253
Methods	POHE	RSWHE	SKHE	FHE	GHE	The proposed EMCE	The proposed EMCE+BP	
Execution time (s)	0.1938	0.8268	1.0047	10.556	0.117	**0.12199**	**0.12576**	

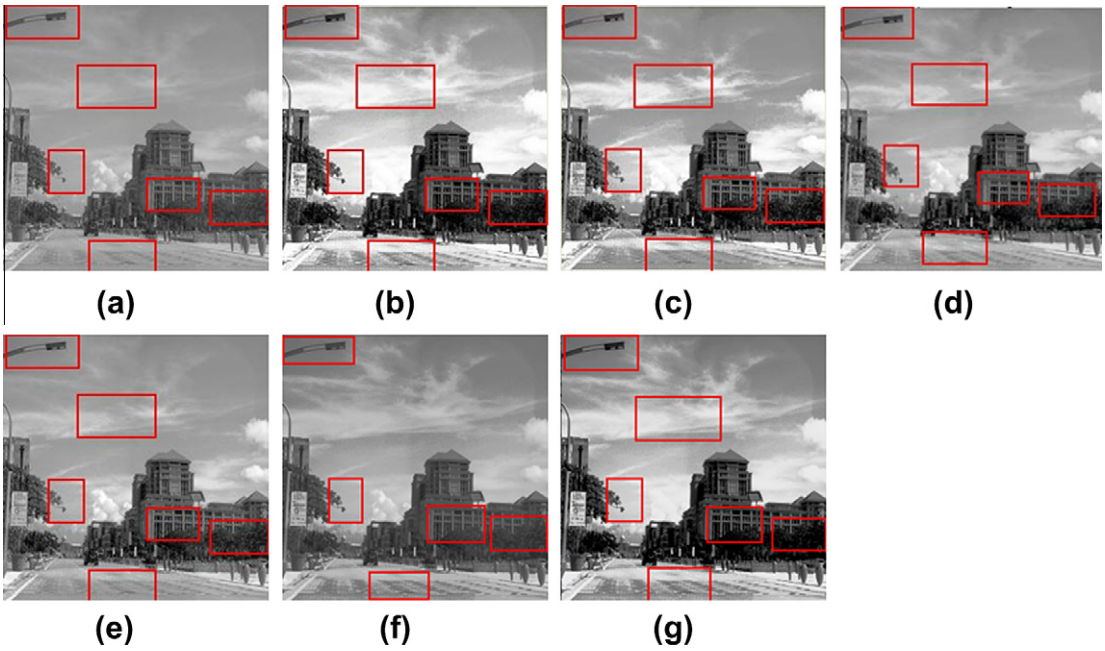

Fig. 6. For image "*Putrajaya*", the results by using mean preserving-based methods. (a) Original image. (b) BBHE. (c) RMSHE. (d) BPDHE. (e) RSWHE. (f) BPWCHE. (g) Our proposed EMCE+BP.

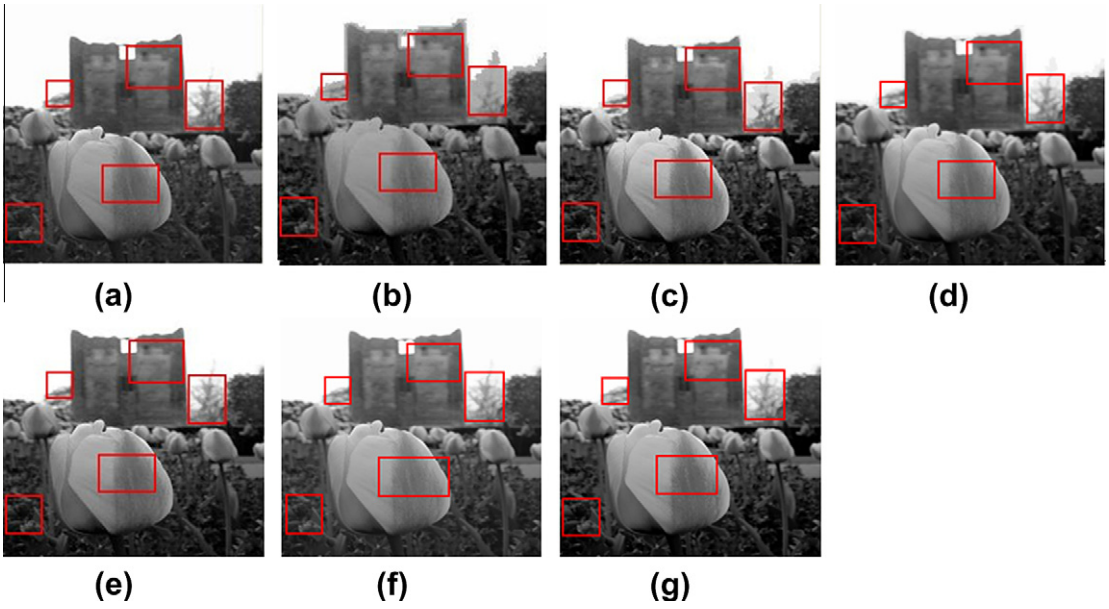

Fig. 7. For image "*Castle*", the results by using mean preserving-based methods. (a) Original image. (b) BBHE. (c) RMSHE. (d) BPDHE. (e) RSWHE. (f) BPWCHE. (g) Our proposed EMCE+BP.

For the second test image "*Castle*", Fig. 4 indicates that the DHE and our proposed EMCE have good contrast enhancement effect. We observe that there are artifacts on the trees at the right side of castle for the HE and the DSIHE. For the RSIHE, the trees and the castle are over-enhanced. The groves enhanced by the GHE and the FHE are some blurred when compared with our proposed EMCE. For the SRHE, some spots appear in the enhanced image.

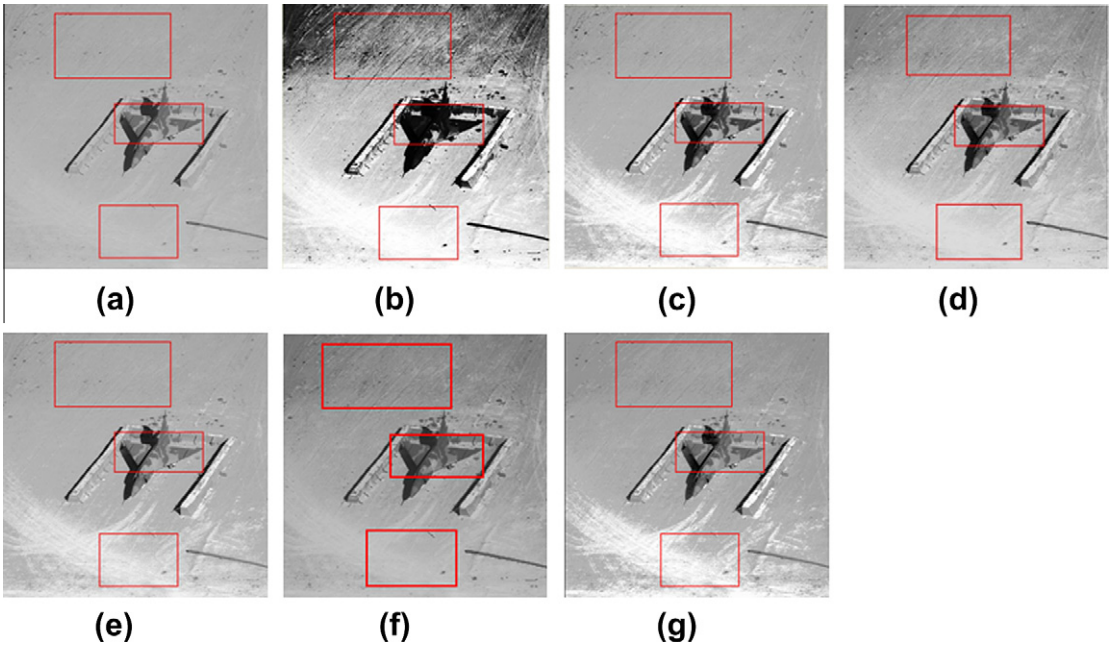

Fig. 8. For image "*Aircraft*", the results by using mean preserving-based methods. (a) Original image. (b) BBHE. (c) RMSHE. (d) BPDHE. (e) RSWHE. (f) BPWCHE. (g) Our proposed EMCE+BP.

For the third test image "*Aircraft*", Fig. 5 indicates that the RSIHE and the proposed EMCE have good contrast enhancement effect on the aircraft body. The RSIHE, the DHE, and the proposed EMCE have good contrast enhancement on the scratch of the ground.

3.3. Subjective comparison of brightness preserving methods

The six concerned brightness preserving methods are evaluated in this subsection. For the test image "*Putrajaya*" as shown in Fig. 6(a), Fig. 6 indicates that our proposed EMCE+BP has competitive contrast enhancement effect (see Fig. 6(g)) on windows of the main building, that between the sky and the clouds, trees in front of the main building and trees at the right side of the left building, the streetlamp, and the main street when compared to the other five existing methods, the BBHE, the RMSHE, the BPDHE, the RSWHE and, the BPWCHE, which are corresponding to Fig. 6(b), (c), (d), (e), and (f), respectively.

For the test image "*Castle*" as shown in Fig. 7(a), from the resultant images in Fig. 7(b), (c), (d), (e), (f), and (g) corresponding to the BBHE, the RMSHE, the BPDHE, the RSWHE, the BPWCHE, and our proposed EMCE+BP, it is observed that besides preserving the details of trees at the right side of the castle, our proposed EMCE+BP has good contrast enhancement effect for the castle and flowers when compared to the BPDHE and the RSWHE.

For the test image "*Aircraft*" as shown in Fig. 8(a), from Figs. 8(b)-(g), it is observed that the RMSHE and our proposed EMCE+BP have good contrast enhancement effect on the scratch of the ground and the aircraft body when compared to the concerned five methods. In addition, the relative contrast between the aircraft body and the ground is rather nature by using our proposed method; however, the stones on the ground are not so apparent. Overall, our proposed method is quite competitive to the four related methods.

3.4. Impact of the threshold parameter

In EMCE+BP, the number of iteration is controlled by the threshold parameter T_{ip} for the Gaussian functions. How to set the threshold T_{ip} properly is an important issue. The smaller the threshold T_{ip} is, the more time is required for algorithm execution. However, the quality of the resulting images will stop improving after the threshold T_{ip} becomes smaller than a certain value.

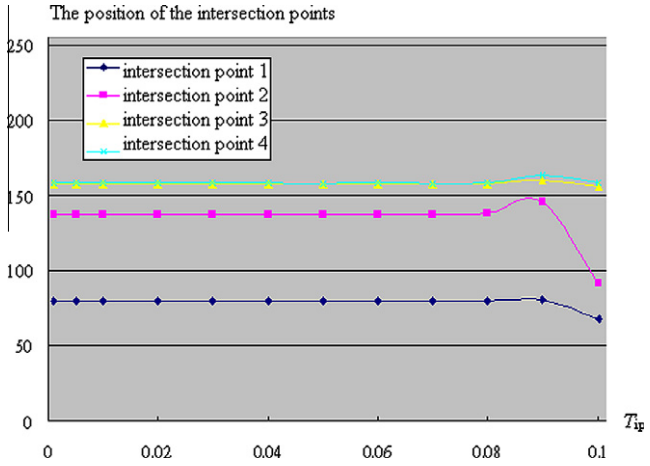

Fig. 9. For image "*Putrajaya*", four intersection points of the histogram is dependent on the threshold T_{ip}.

To understand the the impact of the threshold T_{ip} on quality, we observe the resulting intersection positions that partition the input histogram into sub-histograms. We found that the threshold parameter value of 0.06 is robust across a substantial number of test images. Therefore, the threshold T_{ip} of 0.06 is used in our method.

An example is shown in Fig. 9, which indicates that the discovered intersection positions remain the same after the threshold T_{ip} becomes smaller than 0.06. The resulting contrast enhanced image will be the same afterwards.

4. Conclusion

We have presented a contrast enhancement EMCE+BP method based on Gaussian mixture modeling of image histograms, which provides a sound theoretical underpinning of the partitioning pro-

cess. To the best of our knowledge, this is the first time such an approach is proposed for contrast enhancement. The proposed method contains several novel contributions. First, a scheme for automatic determination of the number of Gaussian function required in a GMM framework is proposed. Secondly, the mixture model provides a nice theoretical framework for histogram modeling. Thirdly, a novel binary search algorithm is proposed to determine the intersection points of adjacent Gaussian functions. Finally, the method includes a brightness preservation operation, allowing it to achieve contrast enhancement while also preserve the natural look of the original images.

Based on three representative test images, experimental results indicate that the performance of EMCE+BP is superior to other relevant methods objectively and subjectively, and is a viable alternative to other methods but with a sound theoretical foundation.

References

Agaian, S. S., Panetta, K., Grigoryan, A. M. (2000). A new measure of image enhancement. In *Int. Conf. Signal Processing Communication* (pp. 19–22).

Cheng, H. D., Xue, M., Shi, X., & Zhang, M. (2007). Novel contrast enhancement approach based on fuzzy homogeneity. *Optical Engineering, 46*(4), 047002.

Chen, S. D., & Ramli, A. R. (2003). Contrast enhancement using recursive mean-separate histogram equalization for scalable brightness preservation. *IEEE Transactions on Consumer Electronics, 49*(4), 1301–1309.

Chen, S. D., & Ramli, A. R. (2003). Minimum mean brightness error bihistogram equalization in contrast enhancement. *IEEE Transactions on Consumer Electronics, 49*(4), 1310–1319.

Ghanekar, U., Singh, A. K., & Pandey, R. (2010). A contrast enhancement-based filter for removal of random valued impulse noise. *IEEE Signal Processing Letters, 17*(1), 47–50.

Gonzalez, R. C., & Woods, R. E. (2002). *Digital image processing* (2nd ed.). Upper Saddle River, NJ: Prentice Hall.

Hartley, H. O. (1958). Maximum likelihood estimation from incomplete data. *Biometrics, 14*(2), 174–194.

Hashemi, S., Kiani, S., Noroozi, N., & Moghaddam, M. E. (2010). An image contrast enhancement method based on genetic algorithm. *Pattern Recognition Letters, 31*(13), 1816–1824.

Ibrahim, H., & Kong, N. S. P. (2007). Brightness preserving dynamic histogram equalization for image contrast enhancement. *IEEE Transactions on Consumer Electronics, 53*(4), 1752–1758.

Ibrahim, H., & Kong, N. S. P. (2009). Image sharpening using sub-regions histogram equalization. *IEEE Transactions on Consumer Electronic, 55*(2), 891–895.

Kang, M., Kim, B., & Sohn, K. (2009). CIECAM02-based tone mapping technique for color image contrast enhancement. *Optical Engineering, 48*(8), 087001.

Kao, W. C., Ye, J. A., Chu, M. I., & Su, C. Y. (2009). Image quality improvement for electrophoretic displays by combining contrast enhancement and halftoning techniques. *IEEE Transactions on Consumer Electronics, 55*(1), 15–19.

Kim, Y. T. (1997). Contrast enhancement using brightness preserving bi-histogram equalization. *IEEE Transactions on Consumer Electronics, 43*(1), 1–8.

Kim, M., & Chung, M. G. (2008). Recursively separated and weighted histogram equalization for brightness preservation and contrast enhancement. *IEEE Transactions on Consumer Electronics, 54*(3), 1389–1397.

Li, Y., Wang, W., & Yu, D. Y. (1994). Application of adaptive histogram equalization to x-ray chest image. *Proceedings of the SPIE, 2321*, 513–514.

Pei, S. C., Zeng, Y. C., & Chang, C. H. (2004). Virtual restoration of ancient Chinese paintings using color contrast enhancement and lacuna texture synthesis. *IEEE Transactions on Image Processing, 13*(3), 416–429.

Pizer, S. M. (2003). The medical image display and analysis group at the University of North Carolina: Reminiscences and philosophy. *IEEE Transactions on Medical Imaging, 22*(1), 2–10.

Sengee, N., & Choi, H. K. (2008). Brightness preserving weight clustering histogram equalization. *IEEE Transactions on Consumer Electronics, 54*(3), 1329–1337.

Sim, K. S., Tso, C. P., & Tan, Y. Y. (2007). Recursive sub-image histogram equalization applied to gray scale images. *Pattern Recognition Letters, 28*(10), 1209–1221.

Torre, A., Peinado, A. M., Segura, J. C., Perez-Cordoba, J. L., Benitez, M. C., & Rubio, A. J. (2005). Histogram equalization of speech representation for robust speech recognition. *IEEE Transactions on Speech Audio Processing, 13*(3), 355–366.

Wadud, M. A. A., Kabir, M. H., Dewan, M. A. A., & Chae, O. (2007). A dynamic histogram equalization for image contrast enhancement. *IEEE Transactions on Consumer Electronics, 53*(2), 593–600.

Wahab, A., Chin, S. H., & Tan, E. C. (1998). Novel approach to automated fingerprint recognition. *Proceedings of IEE Visual Image Signal Processing, 145*(3), 160–166.

Wang, Y., Chen, Q., & Zhang, B. (1999). Image enhancement based on equal area dualistic sub-image histogram equalization method. *IEEE Transactions on Consumer Electronics, 45*(1), 68–75.

Xu, L., & Jordan, M. I. (1996). On convergence properties of the EM algorithm for Gaussian mixtures. *Neural Computation, 8*(1), 129–151.

Zimmerman, J., Pizer, S., Staab, E., Perry, E., McCartney, W., & Brenton, B. (1988). An evaluation of the effectiveness of adaptive histogram equalization for contrast enhancement. *IEEE Transactions on Medical Imaging, 7*(4), 304–312.